Lifetime prediction of laser-precracked fused silica subjected to subsequent cyclic laser pulses

Faiz Dahmani
Laboratory for Laser Energetics and Department of Mechanical Engineering, University of Rochester, 250 East River Road, Rochester, New York 14623-1299

Ansgar W. Schmid
Laboratory for Laser Energetics, University of Rochester, 250 East River Road, Rochester, New York 14623-1299

John C. Lambropoulos
Laboratory for Laser Energetics and Department of Mechanical Engineering, University of Rochester, 250 East River Road, Rochester, New York 14623-1299

Stephen J. Burns
Department of Mechanical Engineering, University of Rochester, 250 East River Road, Rochester, New York 14623-1299

Semyon Papernov
Laboratory for Laser Energetics, University of Rochester, 250 East River Road, Rochester, New York 14623-1299

(Received 13 May 1999; accepted 23 February 2000)

Measurements of fatigue failure strength of laser-cracked fused silica in air at room temperature for different numbers of laser shots and laser fluences are presented. The failure-strength variability is found to be due mainly to the spectrum of crack depths. Agreement with theory suggests the incorporation of a residual term into the failure–strength equation. Due to its sign, the residual stress is of mouth-opening displacement nature at the crack. Analysis of the residual stress data shows a linear proportionality with crack depth, whereas the failure–strength is inversely proportional to the square root of the crack depth.

I. INTRODUCTION

Fused silica has good transparency in the ultraviolet (UV) spectral range; it is widely used as optical-window material in high-fluence, 351-nm positions on glass and 248-nm KrF lasers.[1–5] The useful output of these high-power lasers is limited, however, by laser-induced damage to optical components, including fused silica. Often these optical components (large lenses and windows) separate atmospheric pressure from vacuum areas (10^{-3} to 10^{-4} torr),[1] such as on spatial filters and target tanks, experiencing not only high fluence irradiation conditions but also pressure differential-induced tensile stresses. Under fatigue conditions, i.e., when the strength diminishes for increasing loading duration (here, the number of laser pulses), the damage is initiated by slow crack growth and culminates in catastrophic crack growth and implosive lens or window failure when the stress intensity approaches the critical value.[6,7] Analysis of the strength characteristics then proceeds in accordance with the basic crack propagation equation, i.e., the stress-intensity-factor equation of the form $K \propto \sigma a^{1/2}$, representing the driving force on the crack of characteristic dimension a subjected to an applied stress σ.

Since laser-induced cracks cannot be eliminated entirely, the behavior of cracked structures under service conditions must be quantified to be predicted. Systematic scientific rules must be devised to characterize laser-induced cracks and their effects and to predict if and when it may become necessary to replace the cracked components. This paper makes a contribution toward this end.

Consider a structure in which a laser-induced crack develops. Upon application of repeated laser pulses,[8] or due to a combination of laser fluences and number of laser pulses,[9] this crack will grow: the deeper the crack, the higher the stress concentration induced by it.[9] This implies that the crack-propagation rate will increase with laser fluence and the number of laser shots, causing a progressive decrease in the strength of the structure. After a certain number of laser pulses, the strength becomes so low that the structure cannot withstand accidental high laser fluences (causing more crack growth that can lead to a critical failure crack size) that may occur in service. From this moment on, the structure is liable to fail. If such accidental, high laser fluences do not occur, the laser-induced crack may continue to grow until the strength becomes so low that fracture occurs even under normal service loading [e.g., vacuum loading (10^{-3} to 10^{-4} torr) for fused-silica vacuum barriers].[1]

This paper presents investigations into the fracture behavior and fatigue life of fused silica over the course of many laser pulses and over a limited laser-fluence range when a laser-induced crack is already present. The residual stress associated with the propagating crack is quantitatively monitored by measuring the optical birefringence in the crack vicinity, and fatigue failure strength is quantified by another, standard technique, i.e., an Instron compression-cage unit using four-point bending. Such an experimental approach is applicable to optical glasses other than silica, as is currently done for BK-7 borosilicate glass irradiated at near infrared (IR) wavelength. Attempts at analyzing the experimental observations for silica rest on a simple fracture-mechanics analysis incorporating a residual term into the material-strength equation and presented in Sec. III. This analysis proves successful in explaining the semiellipticity of the periodically laser-loaded crack shape and the fact that the surface crack length (lateral crack) saturates at a maximum value, whereas the median crack (perpendicular to the specimen surface) lengthens without such saturation for all applied laser fluences in the range of 10 to 35 J/cm^2 (0.5 ns, 351 nm). Throughout this work, damage initiation thresholds are reported for the 1-on-1 mode; i.e., each sample site is irradiated only once.

II. EXPERIMENTAL PROCEDURE

Corning 7940 UV, grade-A fused-silica specimens were used for the experiments reported in this paper. The specimens in the form of $64 \times 13.6 \times 4.3$-mm blocks were ground and pitch polished to "laser quality" (rms $\leqslant$ 10 Å) on the entrance and exit surfaces and to "cosmetic quality" around the edges permitting in situ monitoring of the crack propagation. Before laser irradiation, samples were cleaned by the standard drag–wipe technique used to clean sensitive optical components.

A. Laser irradiation

Nd:glass laser pulses of 500-ps duration at the third-harmonic wavelength (351 nm) were used to irradiate the samples. The UV beam was focused onto each sample's front surface by a 2-m-focal-length, fused-silica lens to a 1.2- to 2(±0.3)-mm-diameter spot. The beam incidence direction was chosen to be $\leqslant 10°$ off-normal to the sample entrance surface to prevent any back-reflection of residual, unconverted infrared light from seeding the amplifier in the backward direction.

Although many earlier studies reported on front-surface damage,[10] surface damage (damage is defined to be any visible, permanent modification to the probed surface, observable as scatter sites under a microscope) on fused-silica spatial-filter lenses in OMEGA, Nova, and Beamlet lasers[1–4] occurs first on the input-lens vacuum side, i.e., the lens's exit surface. When a laser beam passes at nearly normal incidence through a transparent sample whose surfaces have been identically prepared, the exit surface suffers a lower damage threshold than the front surface. The optical damage fluences are in fact equal for both surfaces, once reflections and phase shifts of the optical fields at each interface are taken into account. For a perfect sample with refractive index n, the ratio of exit to entrance damage thresholds is $F_{\text{exit/th}}/F_{\text{entrance/th}} = (n+1)^2/4n^2$.[11] A standing wave is formed with a constructive energy-density maximum at $\lambda_L/2$ (where λ_L is the laser wavelength) in front of the surface. This usually results in the formation of a plasma at this point. In the case of the entrance surface, this plasma occurs in air, shielding the sample by absorbing and refracting the incident fluence. At the exit surface, the standing-wave intensity enhancement occurs inside the material, thus increasing the damage initiation probability; therefore, in this work we focus only on the exit-surface damage.

Samples were mounted on a stable x–y translation stage, which shuttled them between the laser-beam path and a 110×-dark-field microscope, such that the irradiated area was automatically in the field of view, permitting identification of small changes in surface morphology and/or modification to the bulk after each irradiation. Fresh sample sites were irradiated on each shot, with the fluence increasing stepwise until damage was observed.

The damage threshold was defined as the arithmetic average of the highest nondamaging fluence and the lowest damaging fluence levels, averaged over a statistical number of irradiation sites per sample surface.

B. Initiation and growth of laser-induced cracks

Once the exit-surface, laser-induced damage threshold ($F_{\text{exit/th}}$) is determined, a flaw (damage initiated at the damage threshold) is deliberately initiated at the specimen center at $F_{\text{exit/th}}$. The created flaw is subsequently irradiated with different number of laser shots at constant laser fluence $F_L > F_{\text{exit/th}}$. After approximately 50 laser shots (depending on the laser fluence used), crack growth initiates. The crack starts propagating toward the front surface as the number of laser shots increases. Efforts are made to avoid front-surface damage (once front-surface damage initiates, a front-surface crack can initiate and propagate, preventing any further laser energy from reaching the exit surface; the exit-surface crack stalls). For this purpose, the laser fluence used is kept below the value of $F_L = 2.5F_{entrance/th}$ (where $F_{entrance/th} = 15.6$ J/cm^2 is the measured entrance-surface damage threshold). Laser fluences of $F_L/F_{exit/th} = 1.8$, 2.2, 2.44, 3, 3.3, and 3.7 are chosen to study the crack propagation under repetitive laser shots.

C. Residual stress field

Fused silica is a material that is neither naturally birefringent nor optically active; however, birefringence may be induced by the presence of stress associated with a crack, as is the case here. Effectively, when a laser-induced crack is initiated after a number of laser shots at a laser-fluence level $F_L > F_{exit/th}$, a residual stress field resulting from the mismatch between the crack and the rest of the matrix builds up in the vicinity of the crack.

The residual stress field induced in laser-cracked fused silica was measured with the use of a Soleil compensator, which is an optical device used to provide controllable retardation between the polarization components of an incident beam of light.[13] A low-power, polarized helium–neon (He–Ne) laser beam focused (≈1 mm) at normal incidence onto the exit surface (the HeNe beam propagates parallel to the crack) was used as a light source. Far away from the crack, the compensator was adjusted to act as a full wave plate so that, with the use of a polarizer, minimal light reached the photodetector. When the HeNe beam passed through the crack vicinity, the level of compensator adjustment required to maintain minimal light at the photodetector yielded a direct measure for the induced relative phase shift between the ordinary and extraordinary rays. (Details of the experimental setup can be found in Ref. 9.) Aligning the HeNe beam onto different exit-surface points yields coarse maps of the birefringence magnitude.

D. Fatigue failure measurements

Fused-silica specimens were laser-cracked in air with different numbers of laser pulses at different laser fluences. Using a universal testing machine, specimens were then loaded and failed in four-point flexure, with the laser-cracked surface on the tensile side. An inner span of 20 mm, an outer span of 32 mm, and a crosshead speed of 0.5 mm/min were used. Applied loads were monitored by a 500-kg load cell, while displacement measurements were made possible by the use of a liner variable differential transformer (LVDT). (Details of the experimental setup can be found in Ref. 8.) Strength values were calculated from the fracture loads and specimen dimensions, using simple beam theory. After strength testing, each specimen was examined optically to ensure that the failure originated from the crack site; those that did not were excluded from the data. To estimate the modulus of rupture of nondamaged fused-silica 7940-UV used here, five nondamaged specimens were also tested. The dimensions of the cracks were obtained from the fracture surface by light microscopy.

III. FRACTURE MECHANICS ANALYSIS

According to fracture-mechanics considerations, a crack will grow catastrophically when the stress intensity, K_I, reaches a critical value, K_{IC} ($K_{IC} = 0.75$ MPa m$^{1/2}$ for fused silica). For a surface flaw in bending, K_{IC} is given by[14]

$$K_F = K_{IC} = \sigma_F \frac{m_b}{\phi} \sqrt{\pi a} \quad , \tag{1}$$

where σ_F is the measured failure strength, a is the crack depth, and m_b and ϕ are numerical factors related to crack and specimen geometry in pure bending, specifically the ratio of crack depth a to specimen thickness t[15]

$$m_b = 1.123 - 1.39\left(\frac{a}{t}\right) + 7.3\left(\frac{a}{t}\right)^2 - 13.1\left(\frac{a}{t}\right)^3 + 14\left(\frac{a}{t}\right)^4 \quad , \text{ for } 0 \leqslant a/t \leqslant 1, \text{ and} \tag{2}$$

$$\phi = \sqrt{1 + 1.46\left(\frac{a}{c}\right)^{1.64}} \quad \text{for } \frac{a}{c} > 1 \quad . \tag{3}$$

The half-surface crack length is c.

Investigations into the nature of laser (or sharp indentation)-induced crack patterns in glass[16–25] have shown that the deformation (crack) zone generally includes an irreversible component,[18,22–25] which becomes manifest as a residual crack driving force in the subsequent failure mechanics.[21] In this case, according to Marshall and Lawn,[18] the total stress intensity factor, K_{tot}, responsible for the crack growth can be written as follows:

$$K_{tot} = K_F + K_R = K_{IC} \quad , \tag{4}$$

with

$$K_R = \frac{\sqrt{\pi a}}{\phi} \sigma_R (m_b + m_t) \tag{5}$$

being the residual stress intensity factor and σ_R being the corresponding residual stress. This residual stress intensity factor has two components, one due to bending and another one due to tension. The numerical factor m_b

due to tension after appropriate simplification (taking into account that fracture is anticipated at $\theta = \pi/2$ for $a/c > 1$) is given by[26]

$$m_t = \left[\sqrt{\frac{c}{a}} \left(1 + 0.04\,\frac{c}{a} \right) + \left(\frac{c}{a} \right)^4 \left(\frac{a}{t} \right)^2 \left(0.2 = 0.11 \left(\frac{a}{t} \right)^2 \right) \right] \left[1.1 + 0.35 \left(\frac{c}{a} \right) \left(\frac{a}{t} \right)^2 \right] \sqrt{\frac{c}{a}} \cong 1.25 \left(\frac{c}{a} \right) \quad . \tag{6}$$

Using Eqs. (1) and (5), Eq. (4) can be rewritten as follows:

$$K_{IC} = \frac{\sqrt{\pi a}}{\phi} \left[m_b \sigma_F + \sigma_R (m_b + m_t) \right] \quad . \tag{7}$$

Using Eq. (7), the residual stress introduced as a result of the laser-irradiation process is calculated for every crack depth a, corresponding to the number of laser shots N and a laser fluence F_L.

IV. RESULTS AND DISCUSSION

A. Dimensions, shape, and crack-growth propagation rate of controlled, laser-induced cracks

The exit-surface damage threshold is found to be $F_{\text{exit/th}} = 10 \pm 0.5$ J/cm^2. The damage at threshold level consists of 1–3-μm conical pits, with larger pits forming at the center of the irradiated area while smaller pits are found in the areas of lower fluence, i.e., in the periphery of the laser beam. Figure 1 shows the exit-surface damage morphology at $F_L = 1.3F_{\text{exit/th}}$ mapped with an atomic force microscope (AFM) at two different magnifications. From Fig. 1(b), it seems that the damage occurred in two stages: an earlier stage corresponding to the absorption of the laser energy by unspecified defects, followed by a localized temperature rise leading to the melting of the matrix surrounding each absorber (defect). The second stage, occurring probably picoseconds later, corresponds to matrix cracking due to steep thermal-stress gradients, a direct consequence of the localized temperature rise. [The AFM used in this mapping is operated outside a clean room. Most of the debris in Figs. 1(a) and 1(b) stems from air and is unrelated to the irradiation].

Micrographs of typical laser-induced crack patterns generated by cyclic laser pulses at a laser fluence of $2.2F_{\text{exit/th}}$ are shown in Figs. 2(a) and 2(b) for $N = 280$ and 430 laser pulses, respectively. Cracks grown in this manner covered a wide range of sizes. The crack depth a and the corresponding crack length c (half-length of the surface trace of the crack) of these cracks were measured by optical microscopy.

(a)
(b)

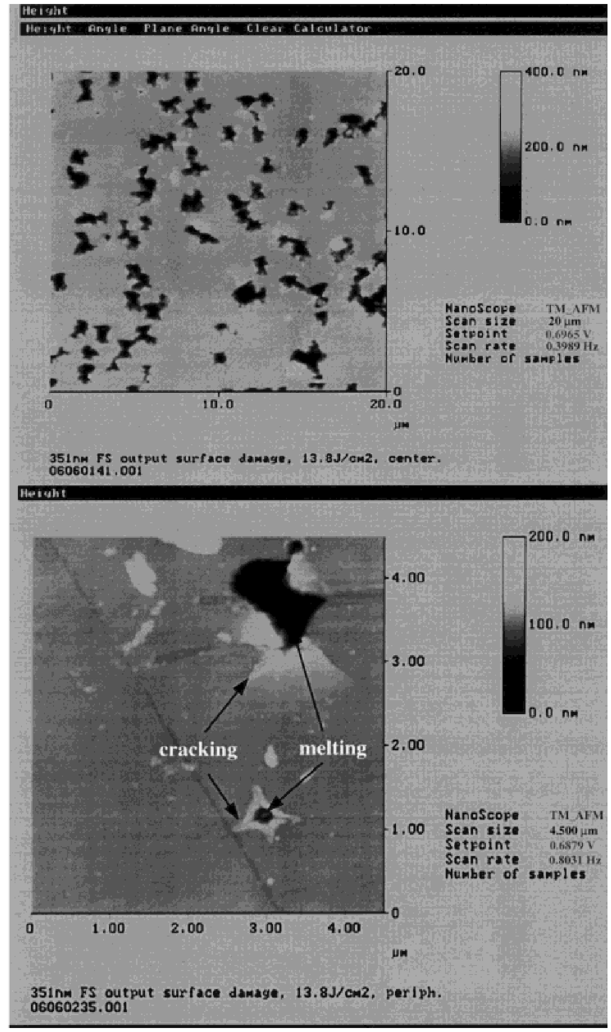

FIG. 1. Fused silica exit-surface 351-nm/500-ps damage (1-on-1 mode) at a laser fluence of $1.38F_{\text{exit/th}}$ mapped with an atomic force microscope (AFM) at two, different magnifications (a), (b). It is clearly seen from the image (b) that the damage occurs in two stages: an earlier stage corresponding to a melting due to the high localized temperatures from the absorption of the laser energy by defects, the second stage corresponding to a cracking, is a direct consequence of the localized high temperatures leading to high thermal stresses.

Cracks were found to be nearly semielliptical in shape. Figure 3 shows the crack-depth data versus the number of laser shots and the laser fluence. It appears from Fig. 3 that the crack depth increases with the number of laser shots and/or laser fluence without apparent saturation. This is true as long as sufficient laser energy is reaching the damage zone. It was observed that when front-surface damage sets in after a given number of laser shots ($N = 300$ to 350) at fluences higher than those used in this work ($F_L/F_{\text{exit/th}} > 3.7$), a front-surface crack initiates and starts propagating toward the exit surface. In

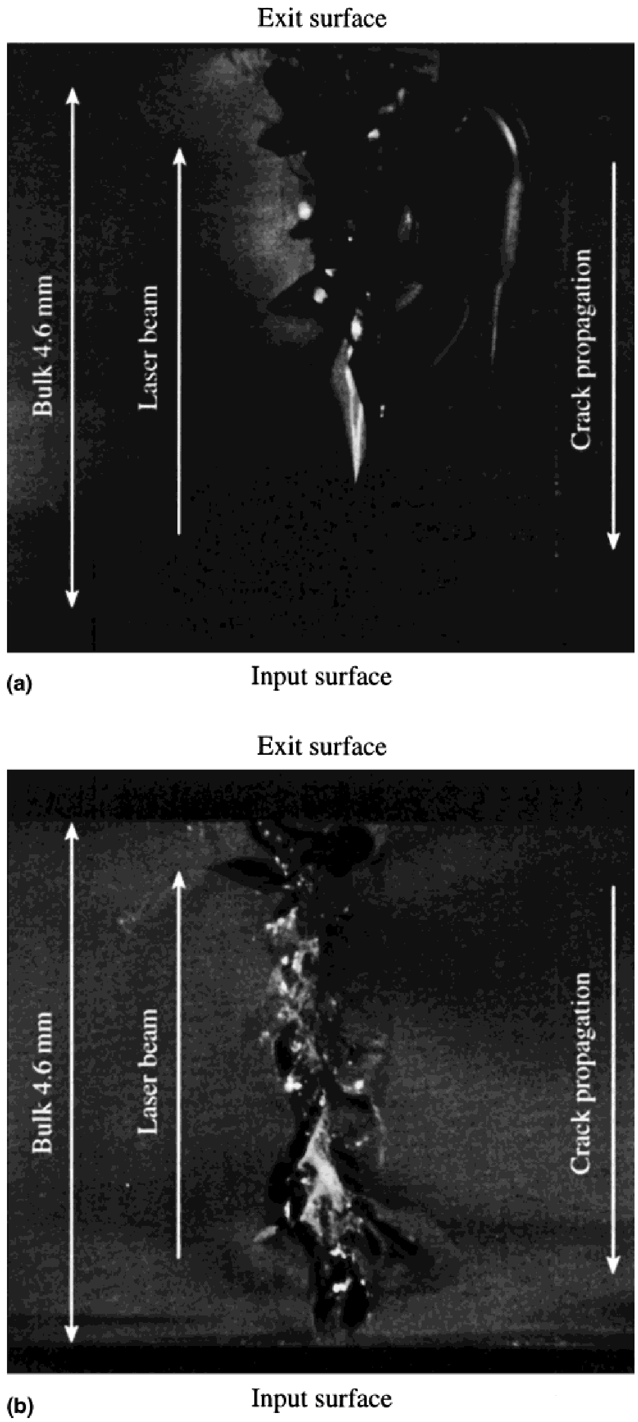

FIG. 2. Cross-sectional view of laser-induced cracks in fused silica at a laser fluence of $F_L = 2.2F_{exit/th}$ for (a) $N = 280$ laser shots and (b) $N = 430$ laser shots. As can be seen, the crack depth increases with the number of laser shots.

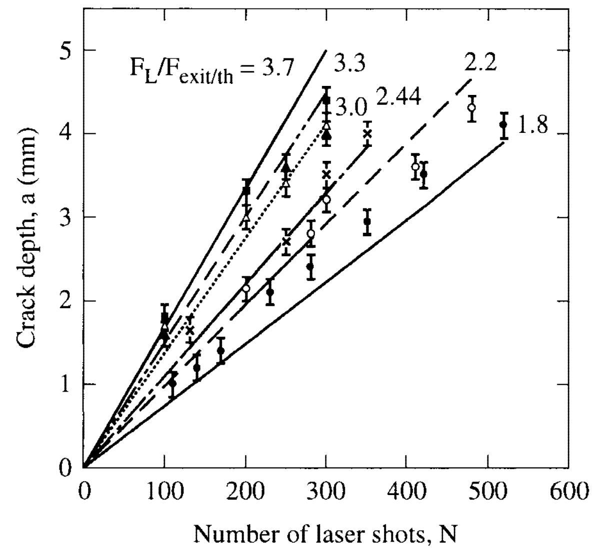

FIG. 3. Crack depth versus the number of laser shots at different laser fluences for fatigue studies. Crack growth rate da/dN is the slope of the data curves. Closed circles are data for $F_L = 1.8F_{exit/th}$, open circles are for $F_L = 2.2F_{exit/th}$, crosses are for $F_L = 2.44F_{exit/th}$, closed triangles are for $F_L = 3.0F_{exit/th}$, open triangles are for $F_L = 3.3F_{exit/th}$, and closed squares are for $F_L = 3.7F_{exit/th}$, respectively. Solid and dashed lines are from Eq. (8).

that event, diminished energy is reaching the rest of the specimen, stalling the back-surface crack growth. As stated previously, care was taken to avoid this situation. On the other hand, after hundreds of laser shots, the crack length c saturates and equals the irradiating beam spot size (0.5 to 1.1 mm), suggesting that the failure strength will depend mainly on the crack depth a.[8] According to the experimental results, a was found to scale with N and F_L as

$$a \cong (8.6 \pm 1.5) \times 10^{-3} N \left(\frac{F_L}{F_{exit/th}} - 1 \right)^{2/3} \quad , \qquad (8)$$

provided $F_L/F_{exit/th} > 1$. It is clearly seen from Eq. (8) that the crack depth is linear in N, which means that the crack growth rate will be independent of N.

As can also be seen from Eq. (8), the fatigue crack rate (da/dN) during laser irradiation of fused silica is only a function of the laser fluence. This crack-growth rate is represented in Fig. 4 versus the laser fluence term $(F_L/F_{exit/th} - 1)^{2/3}$.

B. Determination of residual stress

Prior to fracture strength measurements, the residual stress σ_R was measured for every laser-cracked specimen as a function of crack depth a. This was done by measuring the difference in optical retardation $\Delta\Gamma = \Gamma(\text{crack}) - \Gamma(\text{no crack})$;[9]

$$\sigma_R = \frac{1}{C(\text{nm/cm/MPa})} \frac{\Delta\Gamma\ (\text{nm})}{t(\text{cm})} \quad , \qquad (9)$$

where $C = 35.2$ nm/(cm/MPa)[27] is the relative stress-optic coefficient for fused silica, $\Delta\Gamma$ is the relative retardation, and t is the specimen thickness.

Optical retardation was measured accordingly at defined locations near the cracks, where maxima occurred. Preliminary observations showed that the residual stress field scales with the crack depth *a*. Figure 5 shows the residual stress σ_R (measured at the closest point to the crack, i.e., $r = c + 0.3$ mm, $y = 0$, where c is the half-surface crack length) as a function of the crack depth. The positive sign on the residual stress σ_R, meaning tensile nature of the stresses at the closest point to the crack, suggests a residual mouth-opening displacement at the cracks.

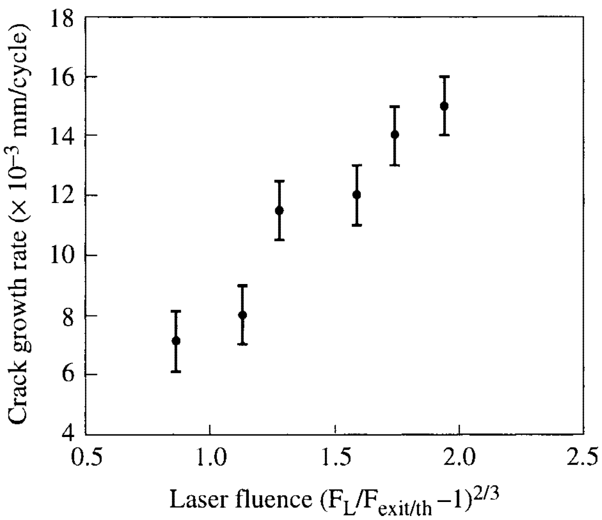

FIG. 4. Fatigue-crack growth rate in laser-cracked fused silica versus laser fluence. Data points are slopes of data points in Fig. 3 for different laser fluences.

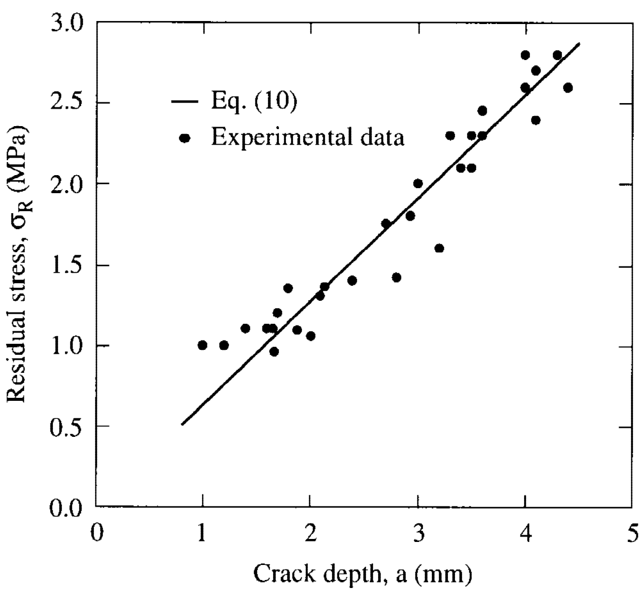

FIG. 5. Residual stress in the vicinity of laser-induced cracks in fused silica versus the crack depth for all laser-cracked fused-silica specimens used in this work. The solid line is from Eq. (10).

In accordance with the experimental data from Fig. 5, the residual stress σ_R can be approximated by the following empirical equation:

$$\sigma_R \text{ (MPa)} \cong 0.64a \text{ (mm)} \quad . \tag{10}$$

C. Failure strength

During the bending tests, specimens without laser-induced crack were fractured into two large and several small pieces and fragments, while specimens with cracks were broken into half-sections at the crack site. The failure strength of nondamaged, polished fused-silica, Corning 7940 samples was measured and found to be (53 ± 2) MPa, which is in good agreement with the value of 50 MPa tabulated by the vendor.[27]

The failure strength data are plotted against the crack depth in Fig. 6. By also plotting the predicted strength from Eq. (1) (solid curve) in Fig. 6, one finds a certain discrepancy becomes apparent between the theory [Eq. (1)] and the experimental data. This discrepancy is alleviated by adding the residual-strength term to Eq. (1) [Eq. (7)], yielding the dashed curve. As can be seen in this figure, the agreement between measured failure strength and the predicted strength is now satisfactory for all crack depths. The σ_F–a data were fitted as suggested by Eq. (7) and are given by

$$\sigma_F \text{ (MPa)} \cong \frac{20}{\sqrt{a \text{ (mm)}}} - 5 \quad . \tag{11}$$

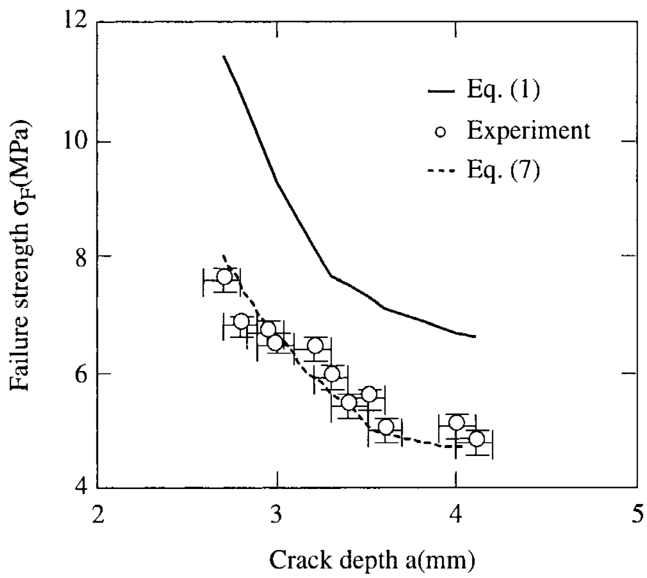

FIG. 6. Failure strength of laser-cracked fused silica as a function of the crack depth *a*. The solid curve is the failure strength calculated from Eq. (1) without residual stress, the dashed curve is the failure strength calculated from Eq. (7), when residual stress in the vicinity of a laser-induced crack is included, and the data points are experimental failure strengths. Good agreement between the experiment and theory is noted when residual stress is included in the formulation of failure strength.

Furthermore, failure strength data are also plotted against the number of laser shots and laser fluences in Fig. 7. It can be noted from this figure that the higher the laser fluence, the smaller the number of laser shots the material is capable of sustaining before failure.

D. Factors affecting fatigue failure

The fatigue failure of fused silica subjected to above damage-threshold laser fluences is highly sensitive to a number of variables. In this work, these factors include laser fluence and number of laser shots as well as residual stress. All these factors are in fact related to one major factor, the crack depth.

1. Laser fluence and number of laser shots

The dependence of fatigue failure on laser fluence and number of laser shots is represented on the σ_F–N plot (Fig. 7). As may be noted, increasing the laser-fluence level and/or the number of laser shots leads to a decrease in fatigue failure of laser-cracked fused silica. For the various experimental conditions, the failure strength σ_F scales with N and F_L as

$$\sigma_F\ (\mathrm{MPa}) \cong \frac{205}{\sqrt{N}\left(\frac{F_L}{F_{\mathrm{exit/th}}-1}\right)^{1/3}} - 5\,\frac{F_L}{F_{\mathrm{exit/th}}} > 1 \quad . \tag{12}$$

2. Residual stress

As seen in Figs. 5 and 6, residual stress and failure strengths increase and decrease, respectively, as the crack depth increases, implying that the residual stress measured around a laser-induced crack in fused silica is a mouth-opening displacement at the radial cracks. Therefore, an increase in residual stress is accompanied by an increase in median crack length (crack depth) as well as a decrease in failure strength. The experimental strengths for laser-cracked fused silica versus residual stress measured around a laser-induced crack, plotted in Fig. 8, support the premise that the weakening of laser-damaged fused silica is adequately described by the increase of residual stress. Our results are in agreement with those of Roach and Cooper[28] for which the reduction in residual stress in Vickers-indented soda-lime glass is accompanied by an increase in failure strength. In the present work, the radial crack length (surface crack length) saturates after a number of laser shots and equals the size of the irradiating beam. The dynamically important parameter is the median crack length (crack depth), on which all measured variables depend.

The σ_F–σ_R curve was fitted to an exponential and is given by

$$\sigma_F\ (\mathrm{MPa}) - 11.85 + 64.48\ \exp(-\sigma_R^{\ 1/3}) \quad , \tag{13}$$

with σ_R given in MPa.

V. CONCLUSION

The fracture patterns of cracks in fused silica, both initiated by and growth-driven by repeated laser shots, were studied. In general, crack shape is best described as a semiellipse. The crack depth, the semiellipse major

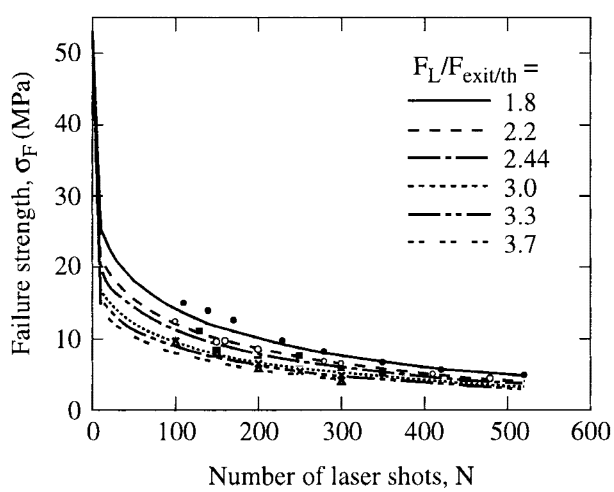

FIG. 7. Failure strength of laser-cracked fused silica versus the number of laser shots. Close circles are data for $F_L = 1.8F_{\mathrm{exit/th}}$, open circles are for $F_L = 2.2F_{\mathrm{exit/th}}$, closed squares are for $F_L = 2.44F_{\mathrm{exit.th}}$, open squares are for $F_L = 3.0F_{\mathrm{exit/th}}$, crosses are for $F_L = 3.3F_{\mathrm{exit/th}}$, and open triangles are for $F_L = 3.7F_{\mathrm{exit/th}}$, respectively. Solid and dashed lines are from Eq. (12).

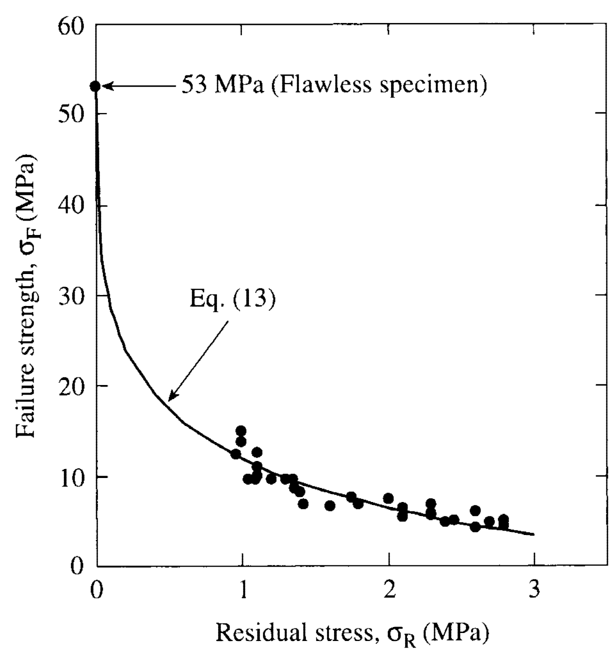

FIG. 8. Failure strength versus residual stress incorporating results from all specimens used in this work. It is evident that residual stress in the vicinity of a laser-induced crack affects dramatically the strength of fused silica. The solid curve is from Eq. (13).

axis, was found to increase with the number of laser shots and/or the laser fluence without apparent saturation as long as no fluence-obscuring, sample front-surface damage was initiated. A theoretical model based on pure-bending-mode failure strength gave good agreement with the experiment when the residual stress was included in the failure strength equation. Any increase in crack depth was accompanied by an increase in residual stress and a decrease in failure strength. The positive sign of the residual stresses measured at the closest point to the laser-induced crack suggested a mouth-opening displacement at the crack.

Both the magnitude and exposure-frequency scale of the strength decrease suggest that the weakening of laser-cracked fused silica is due entirely to residual stress or crack depth increase.

On the basis of our experimental results, an empirical formula for the fatigue-crack growth rate was established, scaling as the two-thirds power of the laser fluence in excess over the damage threshold. This formula contains no fracture-mechanics parameters; it depends only on the laser-fluence level used to irradiate the laser-damaged fused silica. It can be concluded that to minimize the crack growth rate in fused silica subjected to laser irradiation, the laser fluence used must be kept closer to the damage threshold, leading to a longer, useful component life.

ACKNOWLEDGMENTS

This work was supported by the United States Department of Energy (DOE) Office of Inertial Confinement Fusion under Cooperative Agreement No. DE-FC03-92SF19460, the University of Rochester, and the New York State Energy Research Development Authority. The support of the DOE does not constitute an endorsement by the DOE of the views expressed in this article. F. Dahmani is thankful to the Laboratory for Laser Energetics for a F.J. Horton Fellowship. We thank Alex Maltsev for masterfully polishing all sample faces.

REFERENCES

1. J.H. Campbell, P.A. Hurst, D.D. Heggins, W.A. Steele, and S.E. Bumpas, in *Laser-Induced Damage in Optical Materials: 1996*, edited by H.E. Bennett, A.H. Guenther, M.R. Kozlowski, B.E. Newnam, and M.J. Soileau (SPIE, Bellingham, WA, 1997), Vol. 2966, p. 106.
2. J.H. Campbell and F. Rainer, in *Damage to Space Optics and Properties and Characteristics of Optical Glass*, edited by A.J. Marker and J.B. Breckinridge (SPIE, Bellingham, WA, 1993), Vol. 1761, p. 246.
3. J.H. Campbell, G.J. Edwards, and J.E. Marion, in *First Annual International Conference on Solid State Lasers for Application to Inertial Confinement Fusion*, edited by M. André and H.T. Powell (SPIE, Bellingham, WA, 1995), Vol. 2633, p. 522.
4. A.J. Morgan, F. Rainer, F.P. De Marco, R.P. Gonzales, M.R. Kozlowski, and M.C. Staggs, in *Laser Induced Damage in Optical Materials: 1989*, Natl. Inst. Stand. Technol. (U.S.), Spec. Publ. 801 (U.S. Government Printing Office, Washington, DC, 1990), Vol. 1438, p. 47.
5. K. Mann, H. Gerhardt, G. Pfeifer, and R. Wolf, in *Laser-Induced Damage in Optical Materials: 1991*, edited by H.E. Bennett, L.L. Chase, A.H. Guenther, B.E. Newnam, and M.J. Soileau (SPIE, Bellingham, WA, 1992), Vol. 1624, p. 436.
6. S.M. Wiederhorn, H. Johnson, A.M. Diness, and A.H. Heuer, J. Am. Ceram. Soc. **57,** 337 (1974).
7. A.G. Evans, Int. J. Fract. **16,** 485 (1980).
8. F. Dahmani, J.C. Lambropoulos, A.W. Schmid, S. Papernov, and S.J. Burns, J. Mater. Res. **14,** 597 (1999).
9. F. Dahmani, A.W. Schmid, J.C. Lambropoulos, and S.J. Burns, Appl. Opt. **37,** 7772 (1998).
10. D. Albagli, J.A. Izatt, G.B. Hayes, B. Banish, G.S. Janes, I. Itzkan, and M. Feld, in *Laser-Induced Damage in Optical Materials: 1990*, edited by A.H. Guenther, B.E. Newnam, H.E. Bennett, M.J. Soileau, and L.L. Chase (SPIE, Bellingham, WA, 1991), Vol. 1441, p. 146.
11. N.L. Boling, M.D. Crisp, and G. Dubé, Appl. Opt. **12,** 650 (1973).
12. F. Dahmani, Ph.D. Dissertation, University of Rochester (1999).
13. E. Hecht, *Optics*, 2nd ed. (Addison-Wesley, Reading, MA, 1987).
14. J.C. Newman, Jr. and I.S. Raju, Eng. Fract. Mech. **15,** 185 (1981).
15. N. Ingelstrom and H. Nordberg, Eng. Fract. Mech. **6,** 597 (1974).
16. Y.Z. Li, M.P. Harmer, and Y.T. Chou, J. Mater. Res. **9,** 1780 (1994).
17. P.J. Dwivedi and D.J. Green, J. Am. Ceram. Soc. **78,** 2122 (1995).
18. D.B. Marshall and B.R. Lawn, J. Mater. Sci. **14,** 2001 (1979).
19. B.R. Lawn and D.B. Marshall, J. Am. Ceram. Soc. **62,** 106 (1979).
20. D.B. Marshall, B.R. Lawn, and P. Chantikul, J. Mater. Sci. **14,** 2225 (1979).
21. D.B. Marshall and B.R. Lawn, Commun. Am. Ceram. Soc. **No. 1-1,** C-6 (1981).
22. E.R. Fuller, B.R. Lawn, and R.F. Cook, J. Am. Ceram. Soc. **66,** 314 (1983).
23. M.F. Gruninger, B.R. Lawn, E.N. Farabaugh, and J.B. Wachtman, Jr., J. Am. Ceram. Soc. **70,** 344 (1987).
24. R.F. Cook and G.M. Pharr, J. Am. Ceram. Soc. **73,** 787 (1990).
25. K. Zeng and D. Rowcliffe, J. Am. Ceram. Soc. **77,** 524 (1994).
26. M. Isida, H. Nogushi, and T. Yoshida, Int. J. Fract. **26,** 157 (1984).
27. Corning Inc., Advanced Materials Department, Corning, NY.
28. D.H. Roach and A.R. Cooper, J. Am. Ceram. Soc. **68,** 632 (1985).